Journal of Thermal Analysis, Vol. 49 (1997) 1297-1304

A NOVEL PROGRAMMED SHRINKAGE DILATOMETER FOR OPTIMIZED SINTERING OF POWDER CERAMICS

*G. Agarwal, R. F. Speyer and W. S. Hackenberger**

School of Materials Science and Engineering, Georgia Institute of Technology, Atlanta GA 30332
*Center for Dielectric Studies, Materials Research Laboratory, Pennsylvania State University, University Park, PA 16802, USA

Abstract

A fast-firing shrinkage rate controlled dilatometer was developed as a tool for optimizing sintering of powder compacts. The instrument described in this work features an infrared imaging radiation furnace and a low thermal mass dilatometer assembly which allowed controlled heating and cooling rates of up to 500°C min^{-1}. Shrinkage control was accomplished using a computer interfaced PID control algorithm. Adjustments were made to hardware and software which reduced specimen creep under dilatometer pushrod load, eliminated non-uniform pushrod expansion, fostered reproducible specimen temperature determination, accounted for thermal expansion during sintering, and generated instantaneous termination of sintering at the specified end of RCS. Tests performed on ZnO samples demonstrated very rapid thermal response and excellent shrinkage control.

Keywords: dilatometry, rate-controlled-sintering, RCS, sintering, ZnO

Introduction

Rate controlled sintering was first proposed as a method for densifying ceramic materials [1–3]. In this process, furnace power is changed as instructed by a feedback control algorithm to maintain a desired shrinkage rate. The technique was first developed in 1965, and since then, analog control has been supplanted by microprocessor-based systems. Most studies have been carried out using conventional dilatometers. However due to the thermal mass of the furnaces associated with these instruments, the control can be sluggish, restricting the range of possible densification schedules.

Load-induced specimen displacements often provide a supplemental source of shrinkage over and above sintering. Due to simultaneous thermal expansion during sintering, and inability to halt sintering immediately at a specified point, room temperature measured percent shrinkages tend to vary from sample to sample.

Detailed herein is a new system design [4, 5] with a wide variety of unique features which permit appreciably greater flexibility in densification schedule and dimensional control. This system was thus used to provide new insights into the merits of RCS processing. We have used ZnO as the material of investigation since it

0368–4466/97/ $ 5.00

John Wiley & Sons Limited
Chichester

demonstrates a simple solid state sintering mechanism in the temperature range appropriate for this instrument.

Instrument description

The infrared gold image furnace

The infrared image furnace[3] consisted of quartz lamps located at the focal points of elliptical or parabolic mirrors, arranged in such a way that the second focal points of each of the mirrors coincide on to 10 mm diameter center heating zone (Fig. 1). Specimen temperatures as high as 1400°C could be achieved for short times. The specimens were heated solely by radiant energy; there was no insulation in the furnace, and the mirrors which focus the infrared radiation were water cooled.

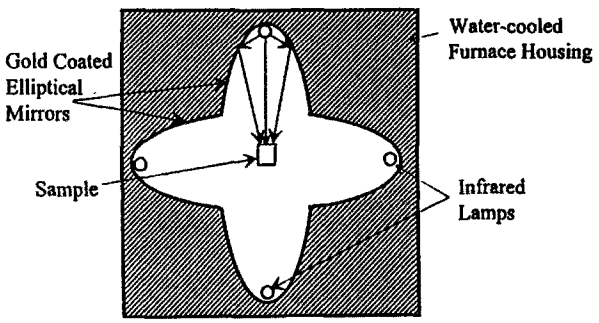

Fig. 1 Schematic cross-section (top-view) of the infrared gold image furnace showing some light paths from the lamp to the sample

The lamps' radiation spectra were approximately that of a blackbody with emission maxima at wavelengths varying from 2 μm at 25% rated power to 1.15 μm at 100% rated power. Controlled heating and cooling rates of up to ~500°C min^{-1} have been demonstrated. This was crucial for RCS experiments where rapid temperature adjustments, both in heating and cooling, were required to meet the more challenging set point densification rates.

Dilatometer assembly and data acquisition

A differential LVDT[4] was used for measuring specimen displacement. The LVDT stage was configured with counter-weighted push rods extending in and out of the furnace in such a way that the system functioned as a double pushrod vertical dilatometer without a casing (Fig. 2). The vertical pushrod design using counterweights was essential to avoid compressive loads from the pushrods which would

3 Model E45P, Ulvac/Siku-Riku Inc., 300, Hakusan-cho, Midoriku, Yokohama, 226, Japan.
4 Dilasoft VIII, Theta Industries, Inc., Port Washington, NY.

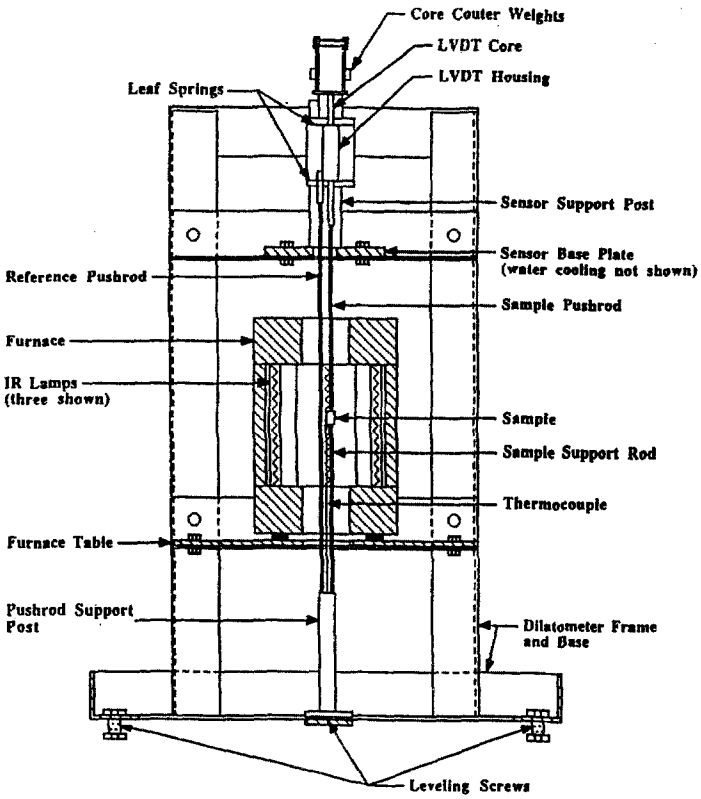

Fig. 2 Front view drawing of the complete dilatometer showing cross-sections of the furnace, base and frame. For clarity, the LVDT assembly, pushrods, and pushrod support post are not shown in cross section

otherwise cause samples to creep. The pushrods contacted 1 mm thick fused silica disks (of diameter greater than specimen diameter) which in turn contacted the specimen on top and bottom.

Data acquisition and furnace feedback control was accomplished using a personal computer with customized software developed in Quick-BASIC[3]. The signals input to the computer control system were the amplified/filtered thermocouple and voltage, thermistor voltage (the latter for cold junction temperature compensation), and the LVDT voltage. These signals were read by an 16-channel 16-bit (76.3 μV precision on a 0–5 V scale) analog to digital (A/D) converter card[4]. After collection and smoothing, the signal bits read by the computer were corrected with experimentally determined amplification factors and standard thermocouple calibra-

3 Microsoft QuickBASIC version 4.5, Microsoft Corporation, N. E. 36th way Redmond Washington 98073.

4 Model CIO-DAS16, Computer Boards Inc., Mansfield, MA.

tion polynomials and converted into appropriate units. Acquired input signals were used by code's proportional-integral-derivative (PID) control algorithm to determine the necessary furnace power level. The operator would program a furnace profile consisting of three separate control regimes. Initially the system operated under temperature control in order to heat the sample to the sintering temperature. The system changed to shrinkage-based control at a user specified switch-over temperature. The specified shrinkage profile could consist of one or two linear shrinkage rates or a shrinkage profile described by a polynomial up to the ninth order. After the end of shrinkage control, temperature control resumed for cool-down at a user-specified rate.

Instrumental modifications for RCS

Specimen creep under load

In the present configuration, the force due to the push rod was minimized by using a vertical system with counterweights. The force applied to the specimen was measured to be 10 g (measured by noting the displacement of a calibrated spring). With this configuration, no creep was observed in specimens after they were sintered, based on dimensional measurements of height and diameter.

Non-uniform pushrod expansion

The intent of the differential pushrod design was to cancel out the expansion of the specimen pushrod by having the expanding/contracting reference pushrod displace the LVDT housing. This necessitated that both pushrods be radially positioned so that they were at the same temperature everywhere along the axis of the furnace, at any given time. In fact, the hot zone of the furnace was not entirely uniform, and this was not a valid assumption; the expansion differences of the pushrods had a measurable effect superimposed on the specimen displacement behavior. As a correction, the alumina pushrods (average CTE: 8×10^{-6} °C^{-1}) were replaced by fused silica pushrods (5.5×10^{-7} °C^{-1}) having a much lower coefficient of thermal expansion. Further, the appreciably lower emittance of the fused silica rods caused them to be at lower temperature than alumina rods exposed to the same radiation levels. The lower temperature rods then would have a lower temperature difference between them, thus a lower expansion difference between them. Thus, the use of fused silica resulted in the elimination of spurious pushrod expansion effects on measured specimen dimensional changes.

Specimen temperature determination

Since the furnace was designed for strictly radiation heating, the specimen was effectively the only absorbing medium in the furnace chamber. The thermocouple junction, having a significantly different thermal mass and a different emittance than the sample, indicated a temperature completely unrelated to the specimen temperature, when placed in close proximity to it. To overcome this problem, the thermocouple was welded to opposite sides of a 0.6 mm thick platinum disc ~0.5 cm in

diameter; this disc was used as a base plate on which the sample was placed and functioned as a virtual thermocouple junction. A correction polynomial was used in the software to correct for the expansion of the platinum disc. This allowed the sample to be in intimate thermal equilibrium with the thermocouple.

Dynamic adjustment for thermal expansion during sintering

Since the feedback control adjusted the power supplied to the furnace in order to achieve the desired shrinkage rate, different temperatures were reached when a specified shrinkage termination criterion had been met. Since the specimen was expanding (due to normal thermally activated dilation) during densification, these differing terminal temperatures fostered differing corresponding expansions.

As a correction, the computer code was designed to make on-the-fly alterations to the time at which RCS was to be halted, to account for thermal expansion of the specimen during sintering. Specimen contraction during RCS was referenced to the point of maximum expansion, generally observed near the end of the heating ramp prior to the onset of RCS. True contractions were continuously recalculated by subtracting calculated expansion from the measured displacement. The calculation of expansion was based on the CTE of the specimen and measured temperature differences. This temperature difference refers to the difference between the value at any point in time during RCS and the value at the aforementioned point of maximum expansion. The CTE of the sample was considered to be constant throughout the RCS temperature range.

After making these adjustments, although the actual shrinkage closely tracked the set point through the first zone, immediate slowing of the densification rate at the onset of the second zone was not feasible. The overshoot in shrinkage rate at switchover was more severe with increasing set point shrinkage rate in the first zone. This occurred despite very rapid temperature adjustments made by the control algorithm. The predominant cause of this problem was the counterproductive effects of specimen thermal contraction: As the furnace temperature control algorithm lowered the temperature to slow the rate of sintering, the cooling specimen contracted, fostering a greater overshoot in measured shrinkage from the set point shrinkage. To counter this effect the control algorithm was programmed to make feedback control adjustments based on corrected contraction rather than measured contraction. Tracking of the set-point was then greatly improved, even when the RCS schedule required a switch-over from an extremely fast shrinkage rate to a slower rate.

Termination of densification after RCS

Initially, a constant cooling rate was specified after termination of RCS, selected so as to not allow thermal shock of the specimen upon cooling. However, these thermal schedules allowed a surprising degree of sintering to continue after termination of RCS. As a correction, a "nosedive" was programmed where the set point was dropped instantaneously by 300°C, followed by a smooth cooling rate, e.g. 50°C min^{-1}. Remarkably, specimen temperature tracked this schedule dutifully. This correction along with the aforementioned CTE correction resulted in very con-

sistent matching between room temperature measured contraction and that specified to the software by the user.

Results and discussion

A typical temperature and expansion profile for the rate-controlled sintering of a ZnO powder compact (6.3 mm diameter, 2.5 mm height with ~65% green density) is illustrated in Fig. 3. During heating from room temperature, the temperature profile in this figure was comprised of two linear regions which were constant heating rates of 100 and 25°C min^{-1} to 750 and 850°C, respectively. Below 100°C, the control was slightly oscillatory, mainly because the radiant heat transfer in this regime was low relative to conduction and convection. Above this temperature, the control was excellent and the actual temperature differed from the set point by less than a degree, even at points where the programmed temperature profile changed slopes.

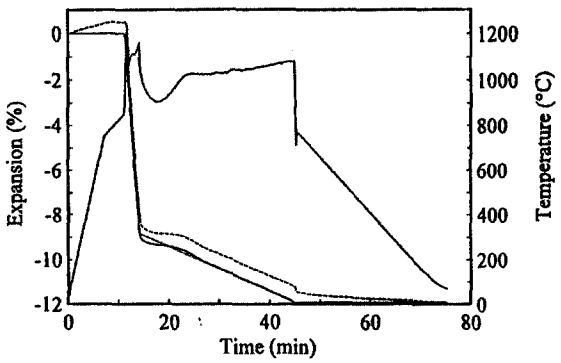

Fig. 3 Dimensional change and temperature profile of a typical rate controlled sintering experiment. Viewing the right hand portion of the graph, the upper solid curve is the temperature profile, and the lower solid curve is the expansion due to sintering. The dotted line corresponds to set point shrinkage rate, and the dashed line is the specimen dilation with no CTE correction

After the switch-over temperature to RCS was reached, the controlled shrinkage schedule began. The feedback control system in conjunction with the rapid heating cooling capabilities of the furnace, demonstrated very rapid temperature adjustments at the beginning of RCS, in order to force specimen shrinkages to match the set point. After the initial adjustments, an increasing temperature trend (with, in some cases, minute superimposed sinusoidal adjustments) was seen, which was required to maintain the set point shrinkage. The actual and set point shrinkage matched each other very well even near the switch-over temperature where the actual and programmed shrinkage rates were very different. A switch-over from fast (0.03 min^{-1}) to slow shrinkage rates (0.001 min^{-1}) took place after 9% total shrinkage. The furnace temperature quickly dropped off until the shrinkage slowed. The

temperature then increased again until the appropriate shrinkage was found. Except for the transition point between the two shrinkage rates, the shrinkage control was excellent throughout the entire RCS schedule. Since the second zone shrinkage rate was slower than the first, a drop in temperature coinciding with the switch-over between zones was apparent. The sudden drop in temperature ("nosedive") stopped further sintering after the total shrinkage of 12% was achieved.

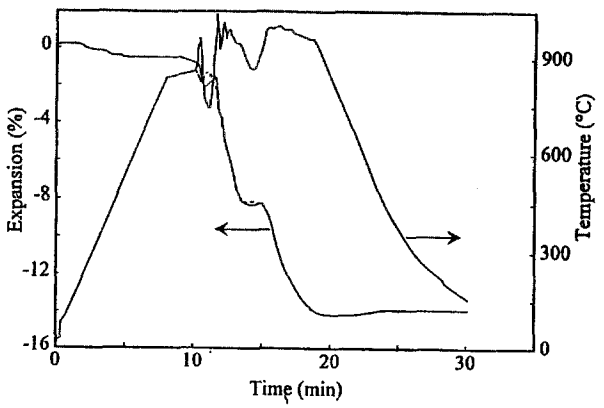

Fig. 4 Rate controlled sintering test of a programmed shrinkage profile described by a ninth order polynomial

Figure 4 shows the results of the polynomial shrinkage profile option. The shrinkage function used was a ninth order polynomial that was determined by digitizing an arbitrary shrinkage curve drawn freehand on a plot of a previously completed rapid linear RCS trial. The polynomial describes a shrinkage curve with two rapid, nearly linear regions connected by a nearly flat shrinkage region. Also, there was slight expansion specified just after the switch-over: As expected, the shrinkage curve did not follow this set point expansion, but the temperature swing in the furnace went through in an attempt to track the set point indicated the rapid thermal responsiveness of the system. The temperature rose from the switch-over value of 855°C to a maximum of 968°C in just 15 s (i.e., a heating rate of about 450°C min^{-1}). It then decreased to 730°C at 370°C min^{-1} and then immediately rose to 1035°C at 485°C min^{-1}. For the remainder of the experiment, the actual value of shrinkage followed the set point remarkably well.

Conclusion

One of the significant advanced demonstrated in this work was the ability to sinter all of the compacts to the same density. This required elimination of pushrod induced creep, on-the-fly correction for thermal expansion during sintering, and instantaneous termination of sintering at a specified shrinkage by a discontinuous temperature drop. The low thermal mass of the furnace and dilatometer assembly allowed the control algorithm to rapidly adjust specimen temperature for the de-

sired shrinkage rate at every instant during the sintering run. The instrument showed a remarkable degree of thermal responsiveness which provided for considerably more control of the sintering process than has been achieved in the past.

References

1 H. Palmour, M. L. Huckabee and T. M. Hare, "Rate Controlled Sintering, Principles and Practice", in Sintering – New Developments, Ed. M. M. Ristic, Plenum Press, New York 1978, pp. 205–15.
2 M. L. Huckabee and H. Palmour, Am. Ceram. Soc. Bull., 51 (1972) 574.
3 H. Palmour, R. A. Bradley and D. R. Johnson, in Kinetics of Reactions in Ionic Systems. Eds T. J. Gray and V. D. Frechette, Plenum Press, New York 1969, pp. 392–407.
4 W. S. Hackenberger and R. F. Speyer, Rev. Sci. Instr., 65 (1993) 701.
5 G. Agarwal, R. F. Speyer and W. S. Hackenberger, J. Mater. Res., 11 (1996) 671.